Available online at www.sciencedirect.com
ScienceDirect
Ceramics International 37 (2011) 3531–3534
CERAMICS INTERNATIONAL
www.elsevier.com/locate/ceramint

Growth and characterization of epitaxial $(La_{2/3}Sr_{1/3})MnO_3$ films by pulsed laser deposition

Dan Liu [a,*], Wei Liu [b]

[a] Materials Research and Education Center, Auburn University, AL 36849, USA
[b] Department of Physics, Wuhan University, Wuhan 430072, People's Republic of China

Received 12 May 2011; received in revised form 7 June 2011; accepted 7 June 2011
Available online 12 June 2011

Abstract

High quality epitaxial $(La_{2/3}Sr_{1/3})MnO_3$ (0 0 1) thin films were grown by pulsed laser deposition on $SrTiO_3$ (0 0 1) substrate at optimized growth parameters. The films quality was confirmed by both structural and physical properties characterization. Channeling Rutherford Backscattering Spectrometry characterization showed the minimal channeling coefficient as low as 4%. The LSMO thin films growth on $SrTiO_3$ substrate follows the island growth model. The Curie temperature of LSMO films is around 360 K, which is the one of the highest reported in literature. The resistivity of LSMO films showed the metal–insulate transition temperature coincides with the Curie temperature. This high quality LSMO is suitable for room temperature magnetic devices application.

Keywords: A. Pulsed laser deposition; A. Epitaxial growth; C. Colossal magnetoresistance; D. LSMO

1. Introduction

The colossal magnetoresistance (CMR) phenomena were observed in many perovskite structure manganite oxide materials. CMR effect was explained by the Zener double-exchange model via Mn^{3+}–O–Mn^{4+} bond [1]. $(La_{2/3}Sr_{1/3})MnO_3$ (LSMO) is one of the most extensively studied CMR materials because its Curie temperature ($T_{c,bulk} \sim 370$ K) is higher than room temperature. This property makes it a great potential candidate in the application of room temperature magnetic devices [2–4].

High quality LSMO thin films are required for the application of magnetic field sensors or magnetic recording devices. Among physical deposition methods, sputtering and pulsed laser deposition are the two most widely used tools in LSMO thin films growth. Compared with sputtering, the PLD has the advantage of growth at wide range of working pressure, from ultra high vacuum to very high gas pressure [5,6]. This advantage is very important for complex composition oxide thin films growth, because the working pressure affects not only the composition, but also the electrical properties of the as-grown films. The electrical properties are modulated through structure, composition and the oxygen vacancies, which are significantly affected by the oxygen working pressure and growth temperature. Besides LSMO [7,8], ferroelectric $(Ba_xSr_{1-x})TiO_3$ [9] and superconducting material $YBa_2Cu_3O_{7-\delta}$ [10] are the successful examples of high quality films growth by PLD.

In this paper, we presented high quality epitaxial growth of LSMO films on single crystal $SrTiO_3$ (0 0 1) substrate. The films quality was proved by both structural and physical properties characterization. The films were systematically studied by Channeling Rutherford Backscattering Spectrometry (c-RBS), secondary electron microscopy (SEM), and physical properties measurement system (PPMS, Quantum Design). The minimum channeling coefficient $\chi \sim 4\%$ was observed by c-RBS, and SEM further showed the epitaxial films follows the island growth model. The measured Curie temperature (T_c) and metal–insulator transition (T_g) temperatures are coincided at 360 K.

2. Experiment

Standard disc shape LSMO target was used in this experiment. Commercial $SrTiO_3$ (0 0 1) single crystal substrate

* Corresponding author. Tel.: +1 334 728 2389.
E-mail address: colin_liud@hotmail.com (D. Liu).

0272-8842/$36.00
doi:10.1016/j.ceramint.2011.06.009

was used for LSMO film epitaxial growth by pulsed laser deposition (PLD). The $SrTiO_3$ substrate was cleaned by acetone, ethanol and DI water in ultrasonic bath, followed by dry nitrogen gas blowing, and then loaded into PLD chamber. The chamber was pumped down to base pressure below 5×10^{-7} Torr. The $SrTiO_3$ substrate was baked in PLD chamber at base pressure at 800 °C for 30 min to further clean the surface trace contamination, and got the surface reconstruction pattern [11]. Before growth, the PLD chamber was filled with oxygen at 350 mTorr pressure and the substrate was cooled down to 600 °C for thin film growth. The target-substrate distance was kept at ~50 mm. During growth, laser power density ~5 J/cm^2 and frequency at 2 Hz was applied to the target. The growth duration was 2.5 h to reach 300 nm thick LSMO films. After growth, LSMO films were cooled down in chamber with oxygen ~10 Torr with cooling rate ~10 °C/min. No further treatment was done on the as-grown LSMO films.

After growth, the structural and physical properties of LSMO films were systematically characterized. The composition and thickness of LSMO films were obtained by Rutherford Backscattering Spectroscopy (RBS). The epitaxial relationship between substrates and films was further characterized by channeling RBS (c-RBS). The surface morphology of the films was observed by SEM. The physical properties, including Curie temperature, temperature–resistivity relationship and coercive force were measured by physical properties measurement system (PPMS, Quantum Design Inc., San Diego, CA).

3. Results and discussion

Channeling Rutherford Backscattering Spectrometry (c-RBS) is a powerful tool to investigate the quality of crystalline materials. Fig. 1 is a typical RBS characterization result of as-grown high quality LSMO films, both random and aligned. The relatively He ion scattering yield (channeling coefficient $\chi \sim 10\%$) near channel 500 (energy 2.7 MeV) is attributed to the LSMO films surface back scattering. The aligned LSMO thin film showed the minimum channeling coefficient $\chi \sim 4\%$, indicating high quality epitaxial LSMO (0 0 1) film on $SrTiO_3$ (0 0 1) substrate. The composition simulation based on RBS spectrum showed the films are stoichiometric $(La_{2/3}Sr_{1/3})MnO_3$, matching that of the target. Generally the composition of as-grown films is affected by the substrate temperature, vapor pressure of each species of the target and working gas pressure. If vapor pressure of one species in the target is significantly different to others, like Zn in $Ba(Zn_{1/3}Ta_{2/3})O_3$ [12], the volatile species Zn will be difficult to be incorporated into the films, compared with less-volatile species (like Ba and Ta), especially at elevated substrate temperature. Oxygen content in the target can always be supplemented since the working oxygen pressure 350 mTorr is high. Similar situation occurred in $Cu(In_xGa_{1-x})Se$ semiconductor thin film growth. High temperature PLD growth of always $Cu(In_xGa_{1-x})Se$ films results in Se-deficiency, and selenization treatment is required to compensate the loss and achieve stoichiometric films [13]. If two or more volatile species in the target, like Zn and As in $ZnGeAs_2$ [14,15], the composition of as-grown films will be very sensitive to the growth temperature. For LSMO, all the metal elements (La, Sr, and Mn) have vapor pressure in the same order of magnitude at 600 °C, which facilitates the high quality thin film growth and the stoichiometry.

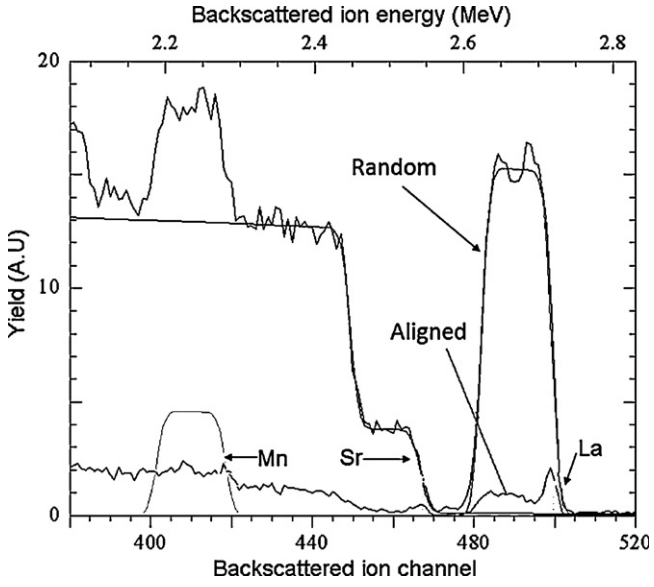

Fig. 1. RBS characterization of LSMO/STO sample, both random and aligned.

Secondary electron microscopy (SEM) was used to observe the surface morphology of PLD grown LSMO films. Fig. 2(A) is the low magnification observation of top films surface, some boulder like feature droplet with size of hundreds nanometers was scattered on the films. This is quite common for PLD films growth, because of the pulsed laser ablates some boulders/particles from the target, and some of boulders was transported through the shock wave in the laser plume, and deposited on the substrate. This non-ideal surface affects the RBS channeling, especially the surface scattering showed in Fig. 1 (surface channeling coefficient $\chi \sim 10\%$). Fig. 2(B) is the high magnification SEM image of the LSMO films. The half micrometer diameter boulder/particle droplet on the films top surface was clearly observed. Besides that, very regular LSMO grains with length ~30 nm square pattern can be observed from the top view. This is very likely that the isolated magnetic domains, when comparing the size and shape reported by Casanove [16]. This surface pattern also showed the epitaxial LSMO growth follows the island growth model, either Volmer–Weber (VW: island formation) or Stranski–Krastanov (S–K: layer plus island growth) model [17]. For VW model, LSMO islands directly grow on STO substrate because of non-wetting. For S–K model, a complete LSMO films with thickness of several monolayers grow in a layer-by-layer fashion on the STO crystal substrate. Beyond the critical thickness, which depends on strain energy and the chemical potential of the deposited LSMO film, the films growth continues through the nucleation and coalescence of adsorbate islands. c-RBS results already showed epitaxial growth of high quality LSMO (0 0 1) films on cubic $SrTiO_3$ (0 0 1) substrate. Considering the similar perovskite structure and lattice constant, the S–K growth model is highly likely for PLD LSMO films growth on $SrTiO_3$

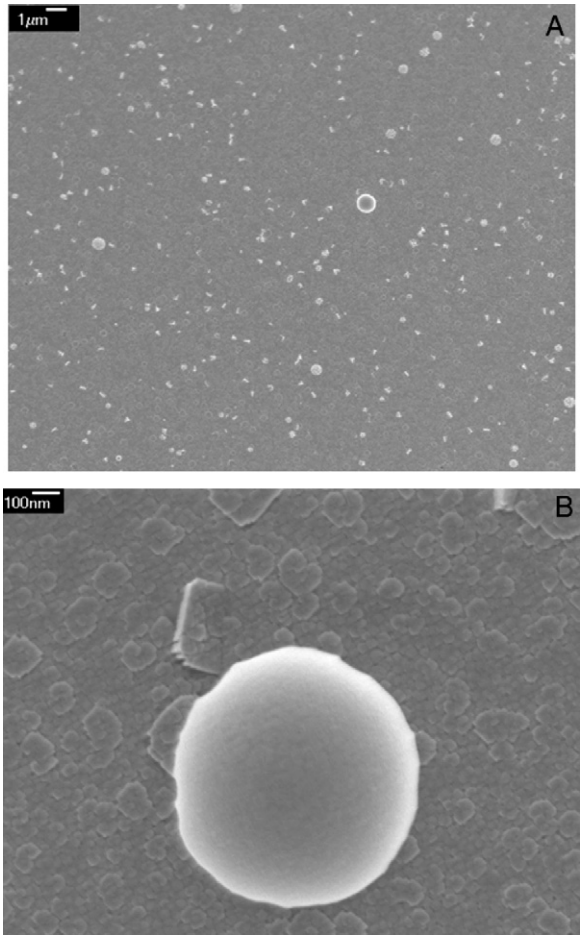

Fig. 2. Low (A) and high magnification (B) SEM observation of as-grown high quality LSMO films on $SrTiO_3$ substrate. The boulder droplet was present on the surface, and the regular square pattern with length ~30 nm was observed on the high magnification (B) image.

substrate. This growth model was observed by high resolution transmission electrons microscopy (HRTEM) [16,18].

The physical properties of as-grown LSMO films were characterized by physical properties measurement system (PPMS, Quantum Design). Fig. 3 shows the magnetic momentum measurement scan from 5 K to 400 K of as-grown LSMO films. During the measurement, 500 Oe magnetic field perpendiculars to the sample surface were applied on the

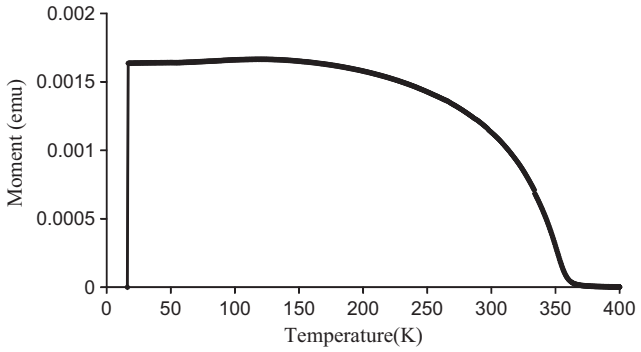

Fig. 3. *M–T* curve to measure Curie temperature of LSMO films.

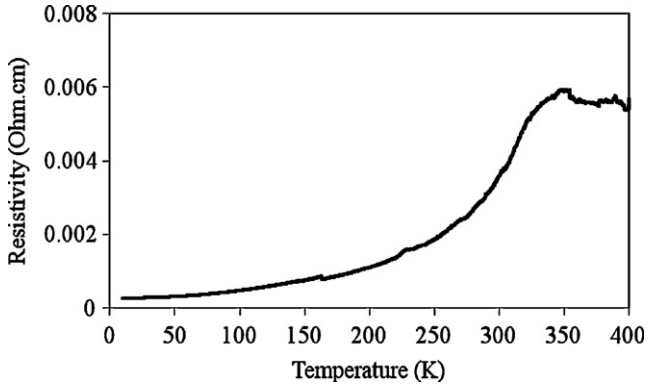

Fig. 4. Resistivity–temperature curve of LSMO sample cooling down from 400 K to 5 K, without magnetic field.

sample. The Curie temperature as high as 360 K was measured, which is close to the bulk LSMO Curie temperature, and is one of the highest in all reported LSMO films [19–21]. The very high Curie temperature further proved the high quality epitaxial films growth by PLD, and makes this films be very useful in room temperature magnetic devices.

The resistivity of as-grown LSMO films as a function of temperature was measured, with and without magnetic field. Fig. 4 is the resistivity–temperature curve of LSMO without magnetic field from 5 to 400 K range (cooling down from 400 K). The metal–insulator transition temperature (T_p) is 360 K, coinciding with the Curie temperature (T_c). This is consistent to the Zener double exchange theory [1]. Experiments already showed when the synthesis in reducing/oxidizing atmosphere could result in the change of T_c and T_p. The possible mechanism is the small variation of oxygen content in the LSMO materials, and it was observed the T_p could be lower [22,23] or higher [24,25] than the T_c. In this experiment, the oxygen working pressure is 350 mTorr. Such a high oxygen pressure could make sure the as-grown films is stoichiometric, and no oxygen deficient, so the coincidence between metal–insulator and ferromagnetic–paramagnetic transition was observed.

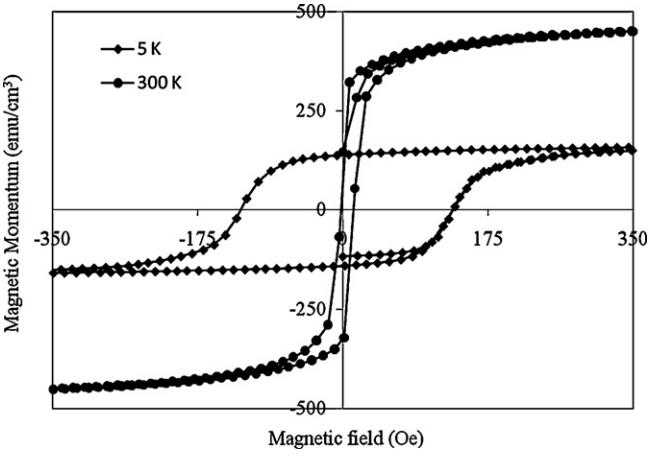

Fig. 5. Typical hysteresis curves of the LSMO films at 300 K and 5 K temperature respectively.

The typical hysteresis curves of the LSMO films at 300 K and 5 K temperature are shown in Fig. 5. The coercive forces are 131 Oe (at 300 K) and 35 Oe (at 5 K), respectively. This value is much lower than typical LSMO films coercive force. For example, the as-deposited LMSO films coercivity at 5 K was reported to be 181 Oe by Du [26], and after 950 °C annealing, the coercivity decreased to 10 Oe, because of the crystalline quality improvement. Generally the defect like surface roughness, grain boundary and point defect all play an important role in determining the coercivity [26,27]. The More defect density, the higher coercivity, because all defects may act as the domain-pining sites. The low coercivity is attributed to the high quality, low defect density of epitaxial LSMO films on STO substrate.

4. Conclusions

Epitaxial $(La_{2/3}Sr_{1/3})MnO_3$ (0 0 1) films have been grown on $SrTiO_3$ (0 0 1) substrate by pulsed laser deposition under optimized growth condition. Both structural and physical properties characterization showed the as-grown LSMO film high quality. The aligned RBS showed the minimal channeling coefficient as low as ~4%, and the measure Curie temperature as high as 360 K. The LSMO top surface regular square pattern showed island growth model. The metal–insulator transition temperature matches the Curie temperature. The relatively low coercivity of as-grown LSMO films proved the high quality epitaxial growth with low defect density. This high quality LSMO films could be very useful for room temperature magnetic devices.

References

[1] C. Zener, Interaction between the d-shells in the transition metals. II. Ferromagnetic compounds of manganese with perovskite structure, Phys. Rev. 82 (1951) 403–405.

[2] C. Moreno, C. Munuera, S. Valencia, F. Kronast, X. Obradors, C. Ocal, Reversible resistive switching and multilevel recording in $La_{0.7}Sr_{0.3}MnO_3$ thin films for low cost nonvolatile memories, Nano Lett. 10 (2010) 3828–3835.

[3] A. Ozbay, E.R. Nowak, Z.G. Yu, W. Chu, Y. Shi, S. Krishnamurthy, Z.Z. Tang, N. Newman, Large magnetoresistance of thick polymer devices having $La_{0.67}Sr_{0.33}MnO_3$ electrodes, Appl. Phys. Lett. 95 (2009) 232507–232509.

[4] O.J. González, E. Castaño, J.C. Castellano, F.J. Gracia, Magnetic position sensor based on nanocrystalline colossal magnetoresistances, Sens. Actuators A 92 (2001) 137–143.

[5] Z.Z. Tang, J.H. Hsieh, S.Y. Zhang, C. Li, Y.Q. Fu, Phase transition and microstructure change in Ta–Zr alloy films by co-sputtering, Surf. Coat. Tech. 198 (2005) 110–113.

[6] D.B. Chrisey, G.K. Hubler, Pulsed Laser Deposition of Thin Films, A Wiley–Interscience Publication, New York, 1994.

[7] M. Koubaa, A.M. Haghiri-Gosnet, R. Desfeux, Ph. Lecoeur, W. Prellier, B. Mercey, Crystallinity, surface morphology, and magnetic properties of $La_{0.7}Sr_{0.3}MnO_3$ thin films: an approach based on the laser ablation plume range models, J. Appl. Phys. 93 (2003) 5227–5235.

[8] F. Pailloux, R. Lyonnet, J.-L. Maurice, J.-P. Contour, Twinning and lattice distortions in the epitaxy of $La_{0.67}Sr_{0.33}MnO_3$ thin films on (0 0 1) $SrTiO_3$, Appl. Surf. Sci. 177 (2001) 263–267.

[9] S. Bandyopadhyay, S.J. Liu, Z.Z. Tang, R.K. Singh, N. Newman, Leakage-current characteristics of vanadium- and scandium-doped barium strontium titanate ceramics over a wide range of DC electric fields, Acta Mater. 57 (2009) 4935–4945.

[10] D.K. Fork, F.A. Ponce, J.C. Tramontana, T.H. Geballe, Epitaxial MgO on Si(0 0 1) for Y–Ba–Cu–O thin-film growth by pulsed laser deposition, Appl. Phys. Lett 58 (1991) 2294–2296.

[11] M.R. Castell, Scanning tunneling microscopy of reconstructions on the $SrTiO_3$(0 0 1) surface, Appl. Surf. 505 (2002) 1–13.

[12] Z.Z. Tang, S.J. Liu, R.K. Singh, S. Bandyopadhyay, I. Sus, T. Kotani, M. van Schilfgaarde, N. Newman, Growth and characterization of epitaxial $Ba(Zn_{1/3}Ta_{2/3})O_3$ (1 0 0) thin films, Acta Mater. 57 (2009) 432–440.

[13] E. Ahmed, A.E. Hill, R.D. Pilkington, R.D. Tomlinson, J. Levoska, O. Kusmartseva, J. Leppävuori, A comparative study of pulsed laser deposition and flash evaporation of $CuLn_{0.75}Ga_{0.25}Se_2$ thin films, Adv. Mater. Optics Electron. 4 (1994) 423–429.

[14] Z.Z. Tang, L. Zhang, R.K. Singh, D. Wright, T. Peshek, T. Gessert, T.J. Coutts, M. van Schilfgaarde, N. Newman, Characterization of $ZnGeAs_2$ thin films produced by pulsed laser deposition, 34th IEEE PVCS (2009) 00437–00439.

[15] T. Peshek, Z.Z. Tang, L. Zhang, R.K. Singh, B. To, T. Gessert, T.J. Coutts, N. Newman, M. van Schilfgaarde, $ZnGeAs_2$ thin films properties: a potentially useful semiconductor for photovoltaic applications, 34th IEEE PVCS (2009) 001367–001369.

[16] M.-J. Casanove, C. Roucau, P. Baulès, J. Majimel, J.-C. Ousset, D. Magnoux, J.F. Bobo, Growth and relaxation mechanisms in $La_{0.66}Sr_{0.33}MnO_3$ manganites deposited on $SrTiO_3$(0 0 1) and MgO(0 0 1), Appl. Surf. Sci. 188 (2002) 19–23.

[17] D.L. Smith, Thin-film Deposition: Principle and Practice, McGraw-Hill Inc., 1995.

[18] O.I. Lebedev, J. Verbeeck, G. Van Tendeloo, C. Dubourdieu, M. Rosina, P. Chaudouet, Structure and properties of artificial $[(La_{0.7}Sr_{0.3}MnO_3)_m(SrTiO_3)_n]_{15}$ superlattices on (0 0 1)$SrTiO_3$, J. Appl. Phys. 94 (2003) 7646–7656.

[19] A.K. Pradhan, D. Hunter, T. Williams, B. Lasley-Hunter, R. Bah, H. Mustafa, R. Rakhimov, J. Zhang, D.J. Sellmyer, E.E. Carpenter, D.R. Sahu, J.-L. Huang, Magnetic properties of $La_{0.6}Sr_{0.4}MnO_3$ thin films on $SrTiO_3$ and buffered Si substrates with varying thickness, J. Appl. Phys. 103 (2008) 023914–023922.

[20] R.D. Averitt, A.I. Lobad, C. Kwon, S.A. Trugman, V.K. Thorsmølle, A.J. Taylor, Ultrafast conductivity dynamics in colossal magnetoresistance manganites, Phys. Rev. Lett. 87 (2001) 017401–017404.

[21] P. Perna, L. Mechin, M.P. Chauvat, P. Ruterana, Ch. Simon, U. Scotti di Uccio, High Curie temperature for $La_{0.7}Sr_{0.3}MnO_3$ thin films deposited on CeO_2/YSZ-based buffered silicon substrates, J. Phys.: Condens. Matter 21 (2009) 306005–306009.

[22] G. De Marzi, H.J. Trodahl, J. Bok, A. Cantarero, F. Sapina, The effect of Cu substitution on the A_{1g} mode of $La_{0.7}Sr_{0.3}MnO_3$ manganites, Solid State Commun. 127 (2003) 259–264.

[23] N. Zhang, S. Zhang, W.P. Ding, W. Zhong, Y.W. Du, Interfacial tunneling and magnetoresistance in granular perovskite $La_{0.82}Sr_{0.18}MnO_z$, Solid State Commun. 107 (1998) 417–422.

[24] R. Bertacco, M. Riva, M. Cantoni, L. Signorini, F. Ciccacci, Epitaxial $La_{2/3}Sr_{1/3}MnO_3$ thin films with metallic behavior above the Curie temperature, Appl. Phys. Lett. 86 (2005) 252502–252504.

[25] G.J. Snyder, R. Hiskes, S. DiCarolis, M.R. Beasley, T.H. Geballe, Intrinsic electrical transport and magnetic properties of $La_{0.67}Ca_{0.33}MnO_3$ and $La_{0.67}Sr_{0.33}MnO_3$ MOCVD thin films and bulk material, Phys. Rev. B 53 (1996) 14434–14444.

[26] M. Pardavi-Horvath, Coercivity of epitaxial magnetic garnet crystals, IEEE Trans. Magn. 21 (1985) 1694–1699.

[27] Y.S. Du, B. Wang, T. Li, D.B. Yu, H. Yan, Effects of annealing procedures on the structural and magnetic properties of epitaxial $La_{0.7}Sr_{0.3}MnO_3$ films, J. Magn. Magn. Mater. 297 (2006) 88–92. http://www.sciencedirect.com/science/article/pii/S0304885305003057.